Spin-polarized tunneling spectroscopy and magnetic coupling in Au-coated Fe/Mo(110) nanostructures

J. Prokop,* A. Kukunin, and H. J. Elmers
Institut für Physik, Johannes Gutenberg-Universität Mainz, Staudingerweg 7, D-55099 Mainz, Germany
(Received 22 January 2007; published 23 April 2007)

We investigated the magnetic properties of epitaxial Au-Fe nanostructures on Mo(110) using spin-polarized scanning tunneling spectroscopy and microscopy at 5 K. Using molecular-beam epitaxy pseudomorphic submonolayer coverages of Au were deposited on Fe/Mo(110) monolayer nanostripes. At 300 K Au atoms nucleate in small islands forming elongated structures along [001]. Annealing at 700 K results in the formation of circular shaped double layer islands in the center of monolayer patches consisting of a homogeneous AuFe alloy. A comparison of tunneling spectra suggests a decomposition of Au and Fe in the double layer islands with Au occupying the top layer. Spin-polarized spectroscopy reveals a small positive spin current asymmetry on Au-coated areas in contrast to large variations observed for the uncovered Fe/Mo(110) monolayer. The lateral indirect exchange coupling between adjacent double layer islands mediated by the bridging AuFe alloy monolayer outbalances the antiparallel dipolar coupling at distances closer than 5 nm.

DOI: 10.1103/PhysRevB.75.144423 PACS number(s): 75.75.+a, 68.37.Ef, 75.60.Ch

I. INTRODUCTION

The investigation of magnetic nanostructures with ultimate lateral resolution using spin-polarized scanning tunneling microscopy provides an enormous impact on the progress of the understanding of magnetism.[1] Direct observation of magnetization structures with atomic resolution and spectroscopy of individual nanostructures[1–4] revealed new insights in magnetic coupling mechanisms, whereas previous investigations of coupling phenomena in nanostructures relied on the investigation of lateral integrated magnetic properties.

Spin-polarized tunneling transport is considered to be extremely sensitive to the interfaces,[5–8] with the transport properties determined primarily by the density of states of the atomic layers directly at the interface.[9,10] The recent discovery of large tunneling magnetoresistance effects in epitaxial tunneling devices has renewed technological and fundamental interest in the tunneling mechanism. For spin-polarized vacuum tunneling inert capping layers are of vital interest. However, the discovery of a tunnel magnetoresistance decaying exponentially with a nominal nonmagnetic interlayer thickness with a length scale of 1–2 Å (Ref. 11) provided a severe obstacle for further investigation of this concept.

In the present paper we focus on heterogeneous nanostructures consisting of the bulk immiscible[12] elements Au and Fe grown on Mo(110).[13] The Fe/Au system has attracted much attention because of self-surfactant effects.[14,15] Although Au is immiscible in bulk Fe,[12] surface alloying has been observed for submonolayer deposition of Au on Fe(001).[16] Conversion electron Mössbauer spectroscopy (CEMS) of ultrathin Fe(001) films grown on Au(001) revealed a considerable AuFe intermixing at the interface accompanied by a formation of a two-dimensional alloy.[17] The magnetic hyperfine field[18] and the magnetic moment[19,20] in the topmost layers of an Fe/Au interface are increased. Monolayer coverages of Au lead to an in-plane spin reorientation of the easy axis of Fe(110)/W(110) films.[21,22]

As a capping material Au is interesting because Au *d* states which may hybridize with the *d* states of the magnetic film are well below the Fermi energy. Therefore one might expect that spin-flip processes of trespassing electrons are suppressed. On the other hand, Au exposes electrons to a large spin-orbit coupling due to its high cardinal number. The observation of magnetization structures in Fe/W(110) through a sulphur overlayer by spin-polarized scanning tunneling microscopy (SP-STM) (Ref. 23) revealed a considerably decreased contrast with unchanged magnetic properties of the underlayer.

Fe/Mo(110) has been chosen as one of the model systems for the scanning tunneling microscopy (STM) and spin-polarized scanning tunneling spectroscopy (SP-STS) studies with well characterized properties.[24–28] The Fe monolayer grows pseudomorphically onto the Mo(110) substrate in the step flow growth forming nanostripes. At low temperature (5 K) the nanostripes are magnetized perpendicular to the surface.[26–28]

In this paper we provide experimental results on two main aspects of heterogeneous Au-Fe nanostructures on Mo(110) and thus considerably extend the preliminary results reported in Ref. 13. The spin-polarized tunneling conductivity through an epitaxial Au monolayer strongly depends on the bias voltage, revealing that one cannot apply a simple model of ballistic transport of electrons from the ferromagnet with some scattering in the nonmagnetic overlayer. Furthermore, we observed an indirect lateral magnetic coupling of adjacent nanostructures.

II. EXPERIMENTAL DETAILS

We prepared the samples in an UHV system (pressure $<1\times10^{-10}$ mbar) using molecular-beam epitaxy (MBE). The Mo(110) single-crystal surface was cleaned using alternating cycles of annealing in oxygen (5×10^{-8} mbar) and flashing at 2000 K.[28] Fe nanostripes grow by step flow growth at 700 K.[24–26,28] Subsequently, a submonolayer coverage of Au was deposited at temperatures between room temperature (RT) and 700 K. Characterization of the samples

involved Auger electron spectroscopy (AES) and low-energy electron diffraction (LEED). For the scanning tunneling microscopy (SP-STM) and spectroscopy (SP-STS) at 5 K we used tungsten tips flashed at 2200 K,[1] and subsequently covered by 10 monolayers (MLs) Au and 4–16 MLs Co at RT with out-of-plane and in-plane magnetic sensitivity.[28] STM images were measured in a constant-current mode at a stabilizing current of 1.5 nA and sample bias of 0.3 V. We performed STM measurements with zero external bias field since the application of external fields was not possible. For simultaneous measurement of differential conductance (dI/dU) maps using a lock-in technique we added a modulation voltage with a frequency of 7 kHz and an amplitude of 30 mV to the sample bias. $dI/dU(U)$ spectra in the range of $U=-1-1$ V were measured with the tip stabilized at 1 V and 1.5 nA.

III. RESULTS AND DISCUSSION

A. Morphology and structure of Au on Fe/Mo(110)

We have grown extended pseudomorphic monolayers (ps-MLs) of Fe by step-flow growth on Mo(110).[28] The ps-ML Fe then serves as a substrate for subsequent deposition of Au. Figure 1 demonstrates the morphology of Au islands on Fe(110)/Mo(110) for submonolayer coverage deposited at room temperature. The simultaneously measured dI/dU maps reveal the different electronic structure of Au on Mo(110) and Au on Fe/Mo(110) by different conductivity values, indicated by the color code. The additional dI/dU contrast enables a clear differentiation of the topology. The morphology of the Au islands is quite different on the pseudomorphic ML Fe(110)/Mo(110) compared to the growth on Mo(110). While Au forms irregular shaped islands on the Mo(110) surface, it aggregates in stripelike structures on Fe that are elongated along [001], indicating an enhanced anisotropic diffusion of Au atoms. An anisotropic diffusion is likely due to the twofold symmetry of the bcc(110) surface. The height of the Au islands on Mo(110) as measured by STM is 0.20 nm, in fair agreement with the bulk lattice constant of Au, whereas the height for Au islands on Fe(110)/Mo(110) is reduced (0.17 nm). However, this reduction can result from the difference in the local density of states rather than from true topographical differences.

LEED images reveal a (1×1) pattern both for Fe/Mo(110) and Au/Fe/Mo(110) as expected for a pseudomorphic growth. The absence of superstructure spots does not necessarily mean that Au grows pseudomorphically, because the Au islands may form incoherent structures. In this case the islands remain too small to diffract electrons into sharp superstructure spots. For Au on 20-ML Fe/W(110) films it is known that Au grows in the Nishiyama-Wassermann orientation at room temperature with the Au(111) plane parallel to the Fe(110) surface and in-plane directions $[1\bar{1}0]$Au$\|$[001]Fe.[21] However, the growth of Au on pseudomorphically strained Fe is likely different. The larger lattice constant might lead to a Kurdjumov-Sachs-like orientation as for the ML Au on Mo(110).[29,30]

At substrate temperatures larger than room temperature during Au deposition or after annealing Au interdiffuses into the Fe monolayer. The amount of interdiffused Au increases with increasing substrate temperature. Both changes of the morphology and variation of the AES spectra before and after annealing indicate the interdiffusion. After annealing at 700 K, the morphology of the Au/Fe/Mo(110) films has changed drastically. Figure 2(a) shows the topography of the sample shown in Fig. 1(e) after annealing. The Mo surface is almost completely covered by an alloy monolayer. On top of the alloy monolayer we observe round shaped islands with a height of 0.15 nm above the Fe ML and an average diameter of 20 mn. The area contribution of the double layer islands is clearly smaller than before annealing revealing the transport of atoms from second layer to first layer sites. Thus an Au-Fe alloy has formed in the first layer. The homogeneous dI/dU signal observed for the alloy monolayer suggests a homogeneous distribution of Au and Fe atoms. The LEED pattern shows a (1×1) pattern similar to the one observed before annealing, indicating that no superstructure is formed during annealing.

For the double layer (DL) islands we propose a structure model with Fe in the first layer and Au in the second layer.

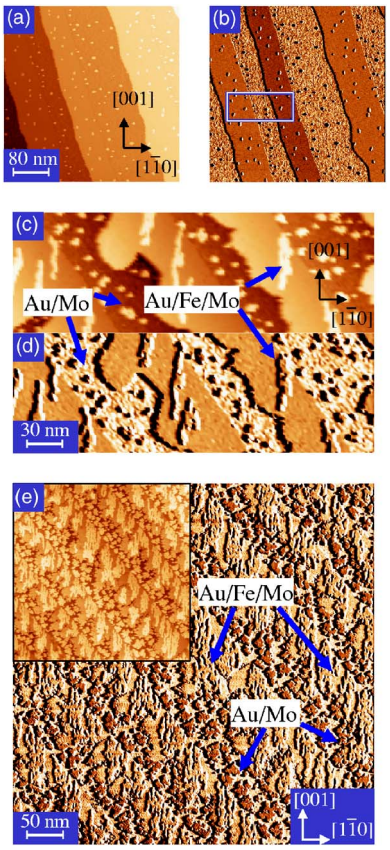

FIG. 1. (Color online) (a) STM image (500×500 nm^2), and (b) simultaneously measured differential conductance dI/dU map of 0.1-ML Au deposited on nanostripes (0.5 ML) Fe/Mo(110). The Fe nanowires separated by uncovered Mo(110) areas reveal an out-of-plane magnetic contrast indicated by different conductivity values. (c) STM image (300×100 nm^2) and (d) simultaneously measured dI/dU map of 0.2-ML Au deposited on 0.5-ML Fe/Mo(110). No magnetic contrast is visible here. (e) dI/dU map (500×500 nm^2) measured for 0.5-ML Au grown on 0.5-ML Fe/Mo(110). Again no magnetic contrast occurs. The inset shows the topography.

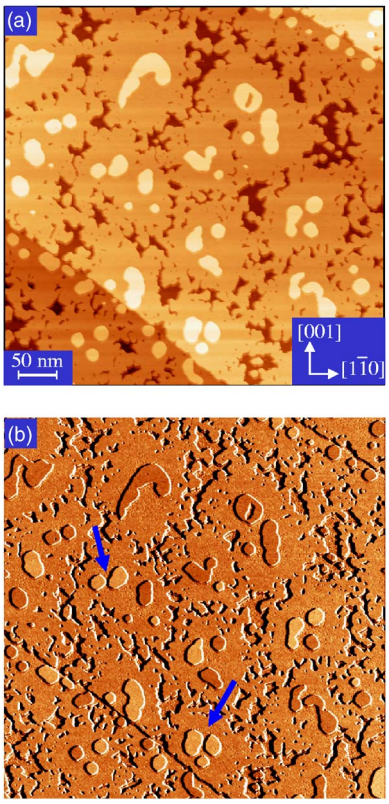

FIG. 2. (Color online) (a) Topography and (b) dI/dU map (500×500 nm^2) for 0.5-ML Au/0.5-ML Fe/Mo(110). The sample is the same as from Fig. 1(e) but measured after annealing at 700 K. The inset (upper left corner) shows the simultaneously measured topography of this surface. Before annealing no magnetic contrast was observed [see Fig. 1(e)]. After annealing, the double layer (DL) islands reveal an out-of-plane magnetic contrast. Islands which are close to each other (indicated by the arrow) are magnetized into the same direction.

This model is suggested by the different values of the free-surface enthalpy [($\gamma_{Mo}=2.9$ Jm^{-2}, $\gamma_{Fe}=2.9$ Jm^{-2}, and $\gamma_{Au}=1.6$ Jm^{-2}) Ref. 31] favoring the Au atoms on top positions and thus minimizing the total free-surface energy of the system. Evaluation of Auger spectra of the inverse sample structure, i.e., a ML Au/Mo(110) covered by a ML of Fe at room temperature, revealed a decrease of the Fe peak and an increase of the Au peak after annealing, thus also supporting the presented model.

The dI/dU map reveals two distinct values on these DL islands. With a nonmagnetic tip only one single value is observed. The two distinct values indicate a magnetic contrast originating from perpendicular magnetized DL islands as discussed below.

B. Magnetic properties

The local conductivity dI/dU measured on the Fe nanowires has two different values, as shown by the different color on the dI/dU map [Fig. 1(b)]. This contrast has a magnetic origin and results from spin-dependent tunneling between the perpendicularly magnetized Fe nanostripes with up and down magnetization direction and the W/Au/Co tip with an out-of-plane magnetic sensitivity.[26–28] This additional magnetic contrast vanishes when the Au coverage exceeds 0.1 ML. This change of magnetic behavior depends solely on the Au coverage occurring simultaneously on wide terraces as shown in Fig. 1, on narrow nanostripes and even on Fe monolayer islands. The vanishing magnetic contrast can be due either to chemical changes of the Fe nanostripe, e.g., interdiffusion of Au or contamination by residual gas adsorption suppressing ferromagnetic order, or to a reorientation of the magnetization direction from perpendicular to in-plane.

Contamination is unlikely because we prepared several samples with different vacuum conditions but similar STS results, however, it cannot be excluded completely. Interdiffusion of Au into the Fe nanostripe requires an interchange of Fe and Au atoms. This interchange provides an energy barrier larger than the thermal energy at room temperature and is therefore suppressed. Mössbauer studies of the similar system Au/ML Fe/W(110) showed that Fe remains at the substrate surface after deposition of Au (Ref. 32) at room temperature. We further determined the percentage of Au-covered Fe ML area from STM images with the result that the percentage agrees with the value expected from the amount of deposited Au as determined by the quartz balance. This observation discards interdiffusion of Au into the Fe ML of more than the experimental error (0.05 ML). We cannot directly exclude smaller amounts of interdiffused Au which then may change the magnetic properties of the Fe ML.

A spin reorientation of the magnetization vector can explain the loss of magnetic contrast. If the magnetization of the sample lies in the surface plane while the magnetization of the tip points perpendicular to the plane, the contrast will vanish. We also measured Au/Fe/Mo(110) samples with tips of in-plane sensitivity without observing a magnetic contrast. For in-plane oriented magnetization the dipolar coupling favors a parallel orientation of adjacent nanostripes in contrast to the antiparallel orientation observed for perpendicular magnetization. Therefore the sample likely comprises a homogeneous magnetization after cooling down preventing the observation of a magnetic contrast for tips with in-plane sensitivity. A strong influence of Au coverages on the magnetic anisotropy is not unlikely. A spin reorientation of the magnetization vector also occurs after deposition of small amounts of Au on thicker Fe/W(110) films.[21,22]

The electronic states localized at the Au atom experience a comparatively large spin-orbit coupling due to the high cardinal number of Au. Therefore even a small hybridization of Fe $3d$ and Au $6s$ states will form polarized states leading to large anisotropic orbital moments and consequently to a large magnetic anisotropy. The Au/Fe(110) interface anisotropy is one of the largest values (–0.47 mJ/m^2).[21] This fact might explain why a small amount of Au has such a dramatic effect on the magnetic anisotropy.

On the annealed Au/Fe/Mo(110) monolayer (Fig. 2) the DL islands are magnetized out-of-plane. The two distinct dI/dU values on these islands indicate the magnetization direction in each island pointing either up or down. The obser-

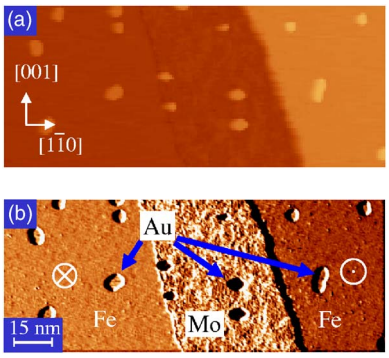

FIG. 3. (Color online) (a) STM image (150×60 nm^2) and (b) dI/dU map of 0.1-ML Au deposited on the 0.5-ML Fe/Mo(110) substrate [magnified part of Figs. 1(a) and 1(b)].

vation of magnetic out-of-plane contrast is surprising since it is in contrast to the vanishing magnetic contrast for Fe/Mo(110) covered by Au at room temperature. As an explanation we suggest either a different local structure of the adsorbed Au atoms similar to the case of Au grown on thicker Fe/W(110) layers[21] or a small amount of Au atoms interdiffused in the Fe layer.

C. Tunneling spectroscopy of Au-covered Fe/Mo(110) monolayers

The magnified part of Figs. 1(a) and 1(b) shown in Fig. 3(b) more clearly reveals the magnetic contrast of the Fe/Mo(110) nanostripes covered by 0.1-ML Au. The local conductivity (dI/dU) on the Au islands is similar to the value on the bare Fe ML. Thus the magnetic contrast at the sample bias of 0.3 V on the Au-covered ps-ML Fe/Mo(110) has almost the same value as observed on the uncovered Fe monolayer.

In order to investigate the dependence of this contrast on the sample bias we measured spectroscopic data on various sample positions. We focused our studies to positive sample bias, i.e., to $-0.2<U<1$ V, where unoccupied states of the sample are probed by occupied tip states. Figure 4 shows spectra from corresponding areas presented in Figs. 1–3 and, for comparison, data from the monolayer and double layer Fe/Mo(110) without Au capping taken from Ref. 28. Although we kept the tunneling parameters constant, the spectra varied slightly, as can be seen, e.g., comparing the spectra from the uncovered and Au covered Fe monolayer which are expected to be identical. This is probably due to varying arrangements of the atoms at the front end of the tip. Accordingly, differences occur in most cases close to zero or at negative sample bias.

The spectra for the Au islands on the ML Fe/Mo(110) show a pronounced peak at 0.65 V and a weak shoulder at 0.15 V for a coverage between 0.1-ML and 0.9-ML Au. Figures 4(c) and 4(e) present data for the lowest and largest coverage. It turned out to be difficult to measure reproducible spectra on the very small Au islands. Unfortunately, it was not possible to gain spin-polarized data on the small Au islands. Larger Au coverages result in reproducible spectra,

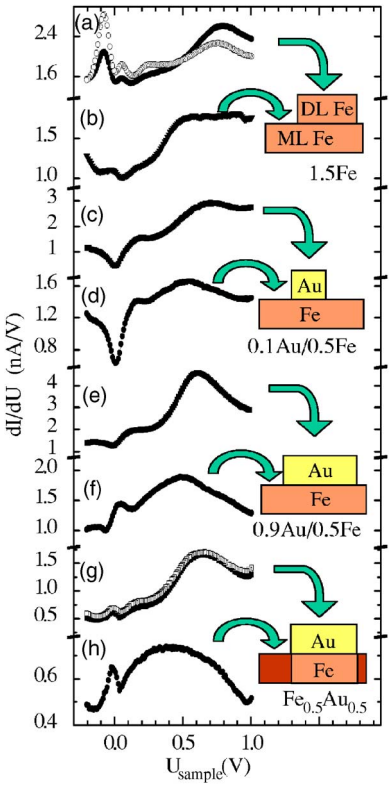

FIG. 4. (Color online) dI/dU spectra measured for 1.5-ML Fe/Mo(110) (a), (b), 0.1-ML Au/0.5-ML Fe/Mo(110) (c), (d), 0.9-ML Au/0.5-ML Fe/Mo(110) (e), (f), and for the 0.5-ML Au/0.5-ML Fe/Mo(110) sample after annealing (g), (h), respectively. Spectra (b), (d), (f), (h) were measured on regions with ML thickness. Spectra (a) (c), (e), (g) were taken on DL areas. Note that the spin-dependent spectra for parallel and antiparallel magnetization orientations of tip and sample are shown in (a) and (g).

however, without magnetic contrast on the sample as discussed above.

Since Au has been deposited at room temperature we expect that spectra measured on the DL islands represent data for a ps-ML Fe covered by a Au ML without intermixing. ML areas in between the Au-covered islands are expected to consist of pure Fe. The spectra [Figs. 4(d) and 4(f)] show a broad peak close to 0.5 V similar to the reference spectra shown in Fig. 4(b), thus confirming the assumed structural model.

Figures 4(g) and 4(h) show spectra of the annealed sample. On the DL islands [Fig. 4(g)] we observe a peak at 0.65 V and a shoulder at 0.2 V, similar to the spectra shown in Figs. 4(c) and 4(e). The spectra of the annealed DL islands are clearly different from the spectra of the DL Fe/Mo(110) shown for comparison in Fig. 4(a). An obvious explanation for the close similarity between spectra Figs. 4(g) and 4(e) is a separation of Fe and Au in the DL islands along the film normal during the annealing procedure with the Fe atoms occupying positions directly at the Mo substrate and Au atoms on top. This is also in agreement with the structure model suggested in Sec. III A.

Homogeneous $Au_{0.5}Fe_{0.5}$ alloy monolayer patches surround the DL islands. Spectra measured on this alloy mono-

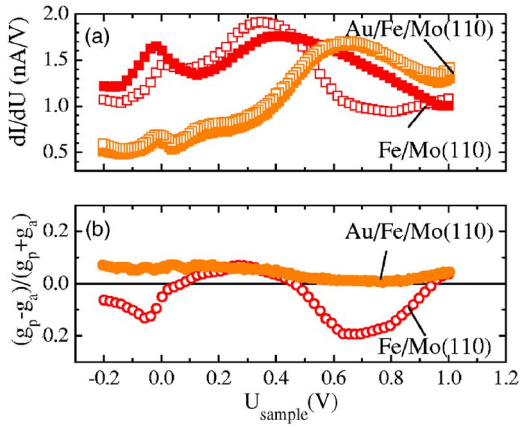

FIG. 5. (Color online) (a) Spin-resolved spectra $(dI/dU)_i := g_i$ for DL islands shown in Fig. 2(b) compared to the corresponding spectra of the ML Fe/Mo(110) (Ref. 28). Open symbols indicate parallel and closed symbols indicate antiparallel orientation of tip and sample magnetization. (b) Asymmetry $(g_p-g_a)/(g_p+g_a)$ of parallel and antiparallel orientation for both cases.

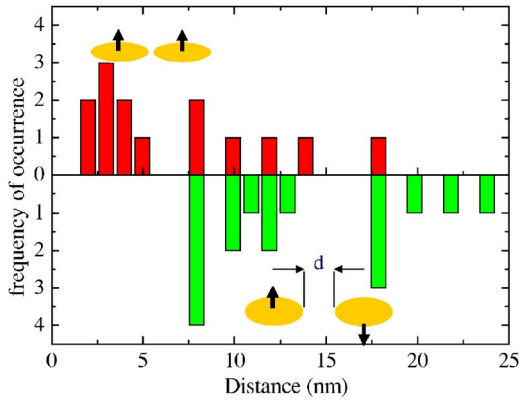

FIG. 6. (Color online) Histogram plot of the occurrence of parallel and antiparallel orientation of the magnetization in DL islands of the annealed Au/Fe/Mo(110) monolayer vs island distance from edge to edge. Data evaluated from Fig. 2(b).

layer [Fig. 4(h)] reveal a very broad feature with a maximum at 0.4 V and are qualitatively different from the spectra of the uncovered Fe ML and the Au-covered Fe ML, thus indicating the different composition.

Spin-resolved spectra measured on the annealed DL islands reveal only a weak asymmetry compared for example with the asymmetry observed for the DL Fe/Mo(110) or ML Fe/Mo(110). Figure 5 shows a direct comparison of spectra on the uncovered ML Fe/Mo(110) with the Au-covered case both measured with the same type of tip. While the asymmetry [Fig. 5(b)] of the bare Fe ML changes sign at 0.1 and 0.5 V, the Au-covered Fe ML reveals only positive values with weak variation. From this observation it is clear that the tunneling spectra cannot be explained by a simple model of electrons starting at the ps-ML Fe and then being transmitted independent of energy through the Au monolayer. The spectra also reveal that the observation of similar contrast on covered and uncovered areas [Fig. 2(b)] at a sample bias of +0.3 V is accidental.

Assuming proportionality between local conductivity and density of states (DOS) we compare our spectra with theoretical predictions. Since band-structure calculations for pseudomorphic Au/Fe/Mo(110) layers have not been performed yet, we take the case of bcc Fe_1/fcc Au_1 multilayers as closest to our system. Reference 20 reported that the d band of Fe dominates the spin-down DOS closely above E_F (0.2 eV) with only a small contribution of $3d$(Fe)-$5d$(Au) hybridization. This might explain the coincidence of the spectra on the uncovered and covered Fe MLs in this energy range.

D. Lateral coupling of islands

For the DL islands of the annealed Au/Fe/Mo(110) sample (Fig. 2) we observe a virgin magnetization state after cooling from above T_c. Thus the magnetization orientation is dominated by the local coupling fields. Adjacent islands are magnetized pairwise antiparallelly in most cases as expected from the dipolar coupling favoring this orientation. However, if the DL islands are very close to each other [indicated, e.g., by the arrow in Fig. 2(b)] the islands are always magnetized in the same direction. In the case of three islands placed closely to each other the dipolar coupling is obviously frustrated.

We counted the number of occurrences of pairwise parallel or antiparallel alignment of islands in Fig. 2(b) as a function of the distance from edge to edge. Figure 6 shows the resulting histogram revealing the exclusive parallel alignment below a distance of 5 nm. Obviously, the antiferromagnetic dipolar coupling is overcompensated by a lateral ferromagnetic exchange coupling. Since the islands are not topographically connected, the coupling must be mediated by the surrounding alloy monolayer.

The energies related to this coupling are very small. The dipolar coupling field of adjacent islands can be estimated to 10^{-3} mJ/m^2 using assumptions as in Ref. 33 and is thus two orders of magnitude smaller than the indirect coupling in multilayers.

IV. CONCLUSIONS

In an effort to reveal spin-polarized transport through an inert nonmagnetic layer we investigated Au-covered Fe/Mo(110) monolayers. Au apparently forms pseudomorphic monolayer islands on the Fe/Mo(110) monolayer. A submonolayer coverage of Au appears as elongated islands along the [100] direction. After annealing at 700 K the system rearranges such that round-shaped double layer islands appear. Tunneling spectroscopy suggests that the DL islands consist of an Fe monolayer capped by an Au layer. A homogeneous AuFe alloy monolayer surrounds the DL islands.

Spin-polarized STM shows that at 5 K the Fe monolayer on Mo(110) maintains an out-of-plane magnetic contrast for Au coverages up to 0.1 ML, while at larger coverage the magnetic contrast disappears. We tentatively attribute this observation to a spin reorientation to an in-plane easy axis. A transition to a paramagnetic behavior due to small amounts

of interdiffused Au provides an alternative explanation. The double layer islands formed during annealing again showed an out-of-plane magnetic contrast.

At a sample bias of 0.3 V the asymmetry of the spin-dependent conductivity is the same on the uncovered and Au-covered Fe/Mo(110) monolayer. Spin-polarized tunneling spectroscopy reveals this fact to be accidental. The sample bias dependence of covered and uncovered areas is different. For the Au-covered Fe monolayer we observe a small positive asymmetry with a minimum at 0.7 V. Contrarily, the uncoated Fe monolayer shows a larger variation with positive and negative values. The conductivity of the bare Fe ML coincides with the corresponding value of Au-covered areas between 0.2 and 0.4 V.

We find a lateral coupling of adjacent DL islands with out-of-plane magnetization comprising a long-range dipolar antiferromagnetic coupling augmented by a short-range indirect ferromagnetic coupling.

ACKNOWLEDGMENT

The financial support of the Deutsche Forschungsgemeinschaft (DFG) is gratefully acknowledged.

*Present address: Max-Planck Institut für Mikrostrukturphysik, Weinberg 2, D-06120 Halle (Saale), Germany.

[1] M. Bode, Rep. Prog. Phys. **66**, 523 (2003).
[2] W. Wulfhekel and J. Kirschner, Appl. Phys. Lett. **75**, 1944 (1999).
[3] S. Heinze, M. Bode, A. Kubetzka, O. Pietzsch, X. Nie, S. Blügel, and R. Wiesendanger, Science **288**, 1805 (2000).
[4] U. Schlickum, W. Wulfhekel, and J. Kirschner, Appl. Phys. Lett. **64**, 2016 (2003).
[5] R. Meservey and P. M. Tedrow, Phys. Rep. **238**, 173 (1994).
[6] J. S. Moodera, J. Nassar, and J. Mathon, J. Magn. Magn. Mater. **200**, 248 (1999).
[7] J. S. Moodera, T. H. Kim, C. Tanaka, and C. H. de Groot, Philos. Mag. B **80**, 195 (2000).
[8] J. M. De Teresa, A. Barthelemy, A. Fert, J. P. Contour, F. Montaigne, and P. Seneor, Science **286**, 507 (1999).
[9] H. Itoh, J. Inoue, S. Maekawa, and P. Bruno, J. Magn. Soc. Jpn. **23**, 52 (1999).
[10] F. Mezei and A. Zawadowski, Phys. Rev. B **3**, 167 (1971).
[11] P. LeClair, J. T. Kohlhepp, H. J. M. Swagten, and W. J. M. de Jonge, Phys. Rev. Lett. **86**, 1066 (2001).
[12] A. R. Miedema, P. F. de Chatel, and F. R. de Boer, Physica B & C **100B**, 1 (1980).
[13] A. Kukunin, J. Prokop, and H. J. Elmers, Acta Phys. Pol. A **109**, 371 (2006).
[14] O. S. Hernán, A. L. Vázquez de Parga, J. M. Gallego, and R. Miranda, Surf. Sci. **415**, 106 (1998).
[15] N. Spiridis and J. Korecki, Surf. Sci. **507-510**, 135 (2002).
[16] M. M. J. Bischoff, T. Yamada, A. J. Quinn, R. G. P. van der Kraan, and H. van Kempen, Phys. Rev. Lett. **87**, 246102 (2001).
[17] W. Karaś, B. Handke, K. Krop, M. Kubik, T. Ślęzak, N. Spiridis, D. Wilgocka-Ślęzak, and J. Korecki, Phys. Status Solidi A **189**, 287 (2002).
[18] M. Przybylski, U. Gradmann, and K. Krop, Hyperfine Interact. **57**, 2045 (1990).
[19] J. A. C. Bland, C. Daboo, B. Heinrich, Z. Celinski, and R. D. Bateson, Phys. Rev. B **51**, 258 (1995).
[20] J. T. Wang, Z. Q. Li, Q. Sun, and Y. Kawazoe, J. Magn. Magn. Mater. **183**, 42 (1998).
[21] H. J. Elmers and U. Gradmann, Surf. Sci. **304**, 201 (1994).
[22] I. G. Baek, H. G. Lee, H. J. Kim, and E. Vescovo, Phys. Rev. B **67**, 075401 (2003).
[23] L. Berbil-Bautista, S. Krause, T. Hänke, M. Bode, and R. Wiesendanger, Surf. Sci. **600**, L20 (2006).
[24] J. Malzbender, M. Przybylski, J. Giergiel, and J. Kirschner, Surf. Sci. **414**, 187 (1998).
[25] S. Murphy, D. Mac Mathuna, G. Mariotto, and I. V. Shvets, Phys. Rev. B **66**, 195417 (2002).
[26] M. Bode, O. Pietzsch, A. Kubetzka, and R. Wiesendanger, Phys. Rev. Lett. **92**, 067201 (2004).
[27] J. Prokop, A. Kukunin, and H. J. Elmers, Phys. Rev. Lett. **95**, 187202 (2005).
[28] J. Prokop, A. Kukunin, and H. J. Elmers, Phys. Rev. B **73**, 014428 (2006).
[29] E. Bauer and H. Poppa, Thin Solid Films **121**, 159 (1984).
[30] A. Pavlovska, M. Paunov, and E. Bauer, Thin Solid Films **126**, 129 (1985).
[31] F. J. Himpsel, J. E. Ortega, G. J. Mankey, and R. F. Willis, Adv. Phys. **47**, 511 (1998).
[32] U. Gradmann, G. Liu, H. J. Elmers, and M. Przybylski, Hyperfine Interact. **57**, 1845 (1990).
[33] M. Pratzer and H. J. Elmers, Phys. Rev. B **66**, 033402 (2002).